Selecting Mechanical Parameters of a Monopode Jumping System with Reinforcement Learning

Andrew Albright¹ and Joshua Vaughan²

Abstract—Legged systems have many advantages when compared to their wheeled counterparts. For example, they can more easily navigate extreme, uneven terrain. However, there are disadvantages as well, including difficulties seen in modeling the nonlinearities of the system. Research has shown that using flexible components is advantageous in terms of both efficiency and legged locomotive performance. Because of the difficulties encountered in modeling flexible systems, control methods such as reinforcement learning can be used to define control strategies. Furthermore, reinforcement learning can be tasked with learning mechanical parameters of a system to match a control input. It is shown in this work that by deploying reinforcement learning to solve for the optimal spring constant and damping ratio for a pogo-stick jumping system, designs which the agent defines are shown to be higher performing in terms of jumping height.

I. Introduction

The use of flexible components within legged locomotive systems has proved useful for both reducing power consumption and increasing performance [1], [2], [3]. However, designing controllers for these systems is difficult as the flexibility of the system generates nonlinear models. As such, employing series-elastic-actuators (SEA) instead of flexible links is an attractive and popular solution, since the models of the systems become more manageable [2], [4], [5]. Still, the use of SEAs do not represent the full capability of flexible systems. As a result, other methods that use flexible tendon-like materials meant to emulate more organic designs have been proposed [6]. These, however, are still not representative of fully flexible links, which have been shown to drastically improve locomotive performance measures such as running speed [7].

Control methods have been developed that work well for flexible systems like the ones mentioned [8], [9]. However, as the systems increase in dimensionality, effects such as dynamic coupling between members make such methods challenging to implement. As such, work has been done that uses neural networks and methods such as reinforcement learning (RL) to develop controllers for flexible systems [10], [11]. For example, RL has been used to create faster running control strategies for flexible-legged locomotive systems that also are robust to different design parameters [12].

In addition to the work done using RL to develop controllers for flexible systems, work has been completed which shows that this technique can be used to concurrently design

the mechanical aspects of a system and a controller to match said system [13]. These techniques have even been used to define mechanical parameters and control strategies where the resulting controller and hardware were deployed in a sim-to-real process, validating the usability of the technique [14]. Using this technique for legged-locomotion has also been studied, but thus far has been limited to the case of rigid systems [15].

As such, this paper starts the discovery of using RL for concurrent design of flexible-legged locomotive systems. A simplified flexible jumping system was used where, for the initial work, the control input was held fixed so that the RL algorithm was tasked with only learning optimized mechanical parameters. The rest of the paper is organized such that in the next section, similar work will be discussed. In Section III, the pogo-stick environment details will be defined. Next, in Section IV, the input used during training will be explained. Then, in Section V, the algorithm used along with the method of the experiments will be explained. The performance of the learned design is presented in Section VI.

II. RELATED WORK

A. Flexible Locomotive Systems

The use of flexible components within locomotive robotics systems has shown improvements in performance measures such as movement speed and jumping height [1], [3]. Previous work has shown that the use of flexible components in the legs of legged locomotion systems increase performance while decreasing power consumption [7]. Related to work on robotics systems employing flexible links, work has been done showing the uses of series-elastic-actuators for locomotive systems [5]. In much of this work, human interaction with the robotic systems is considered where rigidity is not ideal [4]. The studies of flexible systems are challenging however, as the models which represent them are often nonlinear and therefore difficult to develop control systems for. As such, there is a need for solutions which can be deployed to develop controllers for these nonlinear systems.

B. Controlling Flexile Systems Using RL

Control methods developed for flexible linked systems have been shown to be effective for position control and vibration reduction [8], [16]. Because of the challenges seen in scaling the controllers, methods utilizing reinforcement learning are of interest. This method has been used in simple planar cases, where it is compared to a PD control

¹Andrew Albright, Mechanical Engineering Department, University of Louisiana at Lafayette, 320 Rougeau Hall 241 E. Lewis St., Lafayette, LA 70503 andrew.albright1@louisiana.edu

²Joshua Vaughan, Oak Ridge National Laboratory, address email.address@email.com

strategy for vibration suppression and proves to be a higher performing method [17]. Additionally, it has also been shown to be effective at defining control strategies for flexible-legged locomotion. The use of actor-critic algorithms such as Deep Deterministic Policy Gradient [18] have been used to train running strategies for a flexible legged quadruped [12]. Much of the research is based in simulation, however, and often the controllers are not deployed on physical systems, which leads to the question of whether or not these are useful techniques in practice.

C. Concurrent Design

Defining an optimal controller for a system can be difficult due to challenges such as mechanical and electrical design limits. This is especially true when the system is flexible and the model is nonlinear. A solution to this challenge is to concurrently design a system with the controllers so that the two are jointly optimized. This is has been researched in previous work as a strategy to develop better performing mechatronics systems [19]. More recent work has been completed which used advanced methods such as evolutionary strategies to define robot design parameters [20]. In addition to evolutionary strategies, reinforcement learning has been shown to be a viable solution for concurrent design of 2D simulated locomotive systems [13]. This is further shown to be a viable method by demonstrating more complex morphology modifications in 3D reaching and locomotive tasks [15]. However, these techniques have not yet been applied to flexible systems for locomotive tasks.

III. POGO-STICK MODEL

The pogo-stick model show in Figure 1 has been shown to be useful as a representation of several different running and jumping gaits [21]. As such, it is used in this work to demonstrate the ability of reinforcement learning for the mechanical design steps of concurrent design. The model parameters used in the simulations in this paper are summarized in Table I. The variable m_a represents the mass of the actuator, which moves along the rod with mass m_l . A nonlinear spring with constant k is used to represent flexibility within the jumping system. A damper (not shown in Figure 1), is parallel to the spring. Variables x and x_a represent the system's vertical position with respect to the ground and the actuator's position along the rod, respectively. The system is additionally constrained such that it only moves vertically, so the reinforcement agent is not required to balance the system.

The equations of motion describing the system are:

$$\ddot{x} = \frac{\gamma}{m_t} \left(\alpha x + \beta x^3 + c \dot{x} \right) - \frac{m_a}{m_t} \ddot{x}_a - g \tag{1}$$

where x and x_a are position and velocity of the rod respectively, the acceleration of the actuator, x_a , is the control input, and m_t is the mass of the complete system. Constants α and c represent the spring constant and damping constant, respectively, and constant β is set to 1e8. Ground contact

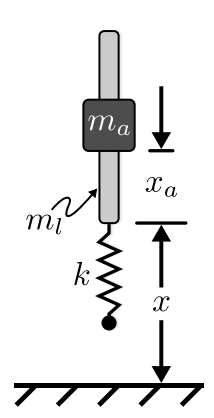


Fig. 1. Pogo-stick System

TABLE I

POGO-STICK MODEL PARAMETERS

Model Parameter	Value		
Mass of Leg, m_l	0.175 kg		
Mass of Actuator, m_a	1.003 kg		
Spring Constant, $k_{nominal}$	5760 N/m		
Natural Frequency, ω_n	$\sqrt{\frac{k}{m_l + m_a}}$		
Damping Ratio, $\zeta_{nominal}$	1e-2 & 7.5e-2 $\frac{N}{m/s}$		
Damping Constant, c	$2 \zeta \omega_n m$		
Actuator Stroke, $(x_a)_{max}$	0.008 m		
Max. Actuator Velocity, $(\dot{x}_a)_{\text{max}}$	1.0 m/s		
Max. Actuator Accel., $(\ddot{x}_a)_{\text{max}}$	10.0 m/s^2		

determines the value of γ , so that the spring and damper do not supply force while the leg is airborne:

$$\gamma = \begin{cases} -1, & x \le 0\\ 0, & \text{otherwise} \end{cases}$$
 (2)

Additionally, a spring compression limit was put in place so that the spring could only compress to a specified amount. For this work, the spring was allowed to compress 0.008 meters as it created varying performance results given the mechanical design choices the reinforcement learning agents were provided.

IV. JUMPING COMMAND DESIGN

Bang-bang derived jumping commands like the one shown in Figure 2 are likely to result in a maximized jump height. For this command, the actuator mass travels at maximum acceleration within its allowable range, pauses, then accelerates in the opposite direction. Commands designed to complete this motion are bang-bang in each direction, with a selectable delay between them. The resulting motion of the actuator along the rod is shown in Figure 3. Starting from an initial position, $(x_a)_0$, it moves through a motion of stroke length Δ_1 , pauses there for δ_t , then moves a distance Δ_2 during the second portion of the acceleration input.

This bang-based profile can be represented as a step command convolved with a series of impulses, as shown in Figure 4 [22]. Using this decomposition, input-shaping principles and tools can be used to design the impulse sequence [23], [24]. For the bang-bang-based jumping command, the amplitudes of the resulting impulse sequence are fixed, $A_i =$

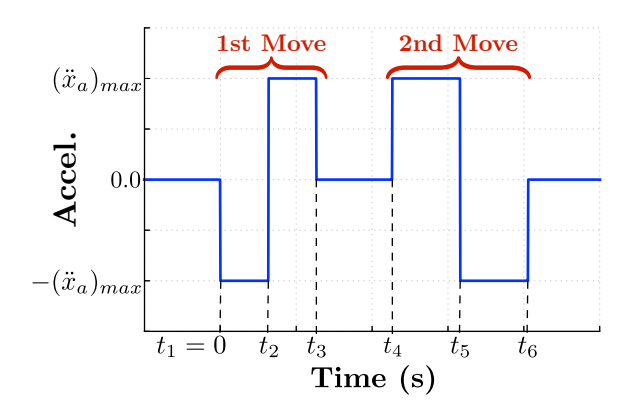


Fig. 2. Jumping Command

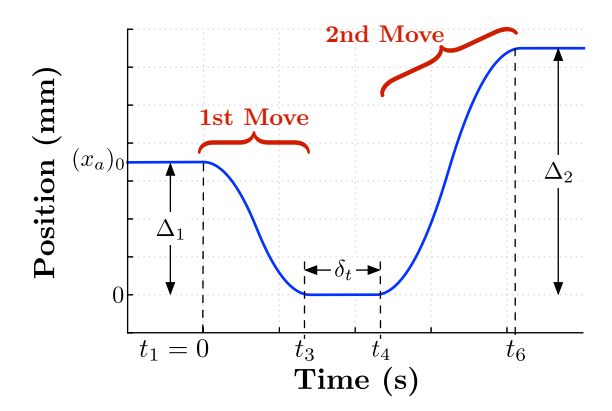


Fig. 3. Resulting Actuator Motion

[-1,2,-1,1,-2,1]. However, the impulse times, t_i , can be varied and optimal selection of them can lead to a maximized jump height of the pogo-stick system [25]. Commands of this form will often result in a stutter jump like that in Figure IV, where the small initial jump allows the system to compress the spring to store energy in the spring to be used in the final jump. This jumping command type was used as the input for the pogo-stick during the simulation phase of training.

V. LEARNING SPRING CONSTANT AND DAMPING RATIO

A. Reinforcement Learning Algorithm

The algorithm used for this work was Twin Delayed Deep Deterministic Policy Gradient (TD3) [26]. This is an actor-critic algorithm wherein there exists two main neural networks and a set of twin trailing networks. The first main network is the actor, which determines the action of the agent. This network takes in the systems state, \mathcal{S} , and outputs the action, \mathcal{A} , based on the state. The critic is an estimator of the value of being in a state and is used to determine the difference between expected and estimated value used to update the actor network during training. It takes in the systems state, \mathcal{S} , and outputs the expected future reward, \mathbb{R} , from being in that state. The twin trailing networks are used to find the temporal difference error against the critic network which is used to update the critic network.

The training hyperparameters were selected based on TD3's author recommendations along with Stable Baselines

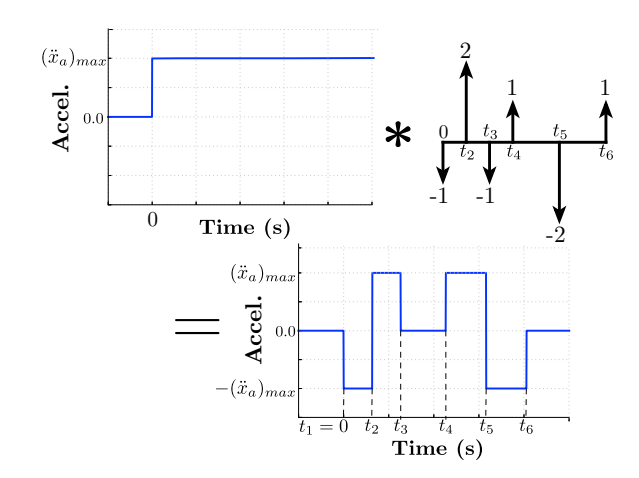


Fig. 4. Decomposition of the Jump Command into a Step Convolved with an Impulse Sequence

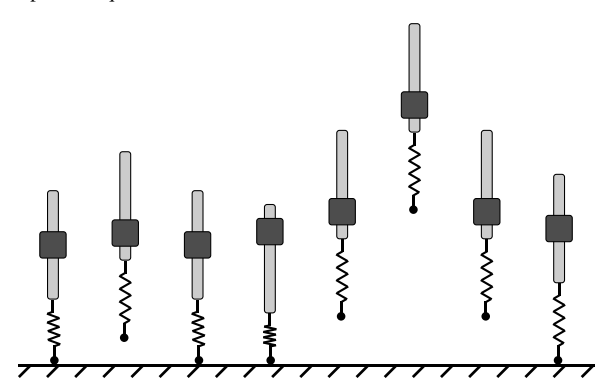


Fig. 5. Example Stutter Jump

experimental findings, and are displayed in Table II. All of the hyperparameters, with the exception of the rollout (Learning Starts) and the replay buffer, were set according to Stable Baselines standards. The rollout setting was defined such that the agent could search the design space at random, filling the replay buffer with enough experience to prevent the agent from converging to a design space that was not optimal. The replay buffer was sized proportional to the number of training steps due to system memory constraints.

B. Training Environment Design

To allow the agent to find a mechanical design, a reinforcement learning environment conforming to the OpenAI Gym standard [27] was created for the pogo-stick model described in Section III, including a fixed controller input based on the algorithm described in the previous section. Unlike the common use case for RL, which is tasking the agent with finding a control input to match a design, the agent in this work was tasked with finding mechanical parameters to match a control input.

The mechanical parameters the agent was tasked with optimizing were the spring constant and the damping ratio of the pogo-stick system. At each time step during training, the agent selected a set of design parameters from a distribution of available designs, that were used to simulate the design

TABLE II
TD3 Training Hyperparameters

Hyperameter	Value		
Learning Rate, α	0.001		
Learning Starts	100 Steps		
Batch Size	100 Transitions		
Tau. τ	0.005		
Gamma, γ	0.99		
Training Frequency	1:Episode		
Gradient Steps			
Action Noise, ϵ	None		
Policy Delay	1:2 Q-Function Updates		
Target Policy Noise, ϵ	0.2		
Target Policy Clip, c	0.5		
Seed	100 Random Seeds		

using the input described in the previous section. The actions applied, A, and transitions saved, S, from the environment were defined as follows:

$$\mathcal{A} = \{ \{ a_k \in \mathbb{R} : [-0.9k, 0.9k] \},$$

$$\{ a_\zeta \in \mathbb{R} : [-0.9\zeta, 0.9\zeta] \} \}$$
(3)

$$S = \left\{ \sum_{t=0}^{t_f} x_t, \sum_{t=0}^{t_f} \dot{x}_t, \sum_{t=0}^{t_f} x_{at}, \sum_{t=0}^{t_f} \dot{x}_{at} \right\}$$
(4)

where k and ζ where the nominal spring constant and damping ratio of the pogo-stick, respectively; x_t and \dot{x}_t were the pogo-stick rod height and velocity steps, and x_{at} and \dot{x}_{at} are the pogo-stick actuator position and velocity steps, all captured during simulation.

C. Reward Function Design

The RL algorithm was utilized to find designs for two different reward cases. Time series data was captured during the simulation phase of training and was used to evaluate the designs performance through these rewards. The first reward case used was:

$$\mathbb{R}_1 = \left(\sum_{t=0}^{t_f} x_t\right)_{max} \tag{5}$$

where x_t was the pogo-stick's rod height at each step during simulation. The goal of the first reward was to find a design that would allow the pogo-stick to jump as high as possible.

The reward for the second case was:

$$\mathbb{R}_2 = \frac{1}{\frac{|\mathbb{R}_1 - x_s|}{x_s} + 1} \tag{6}$$

where x_s was the desired jump height which for this work was set to 0.01 meters. The second case was utilized to test RL's ability to find a design that minimized the error between the maximum height reached and the desired maximum height to reach.

D. Training Schedule

To evaluate the algorithms ability to robustly find design parameters meeting performance needs regardless of the neural network initializations, 100 different agents were trained with different network initialization seeds. Additionally, to verify if RL could be used to find optimal designs given a

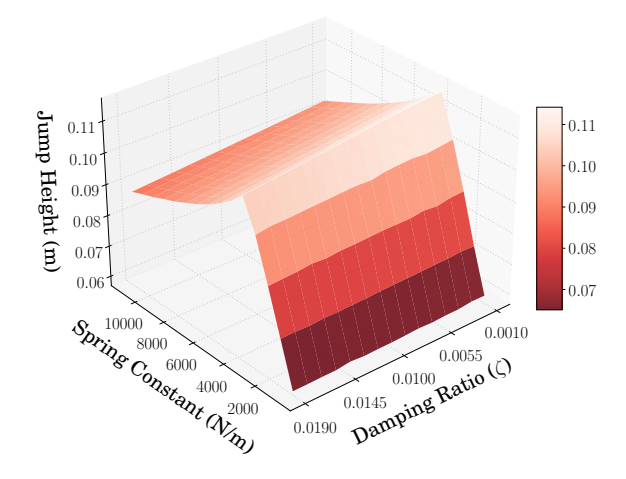


Fig. 6. Height Jumped Given Close to Optimal Range of Design Parameters

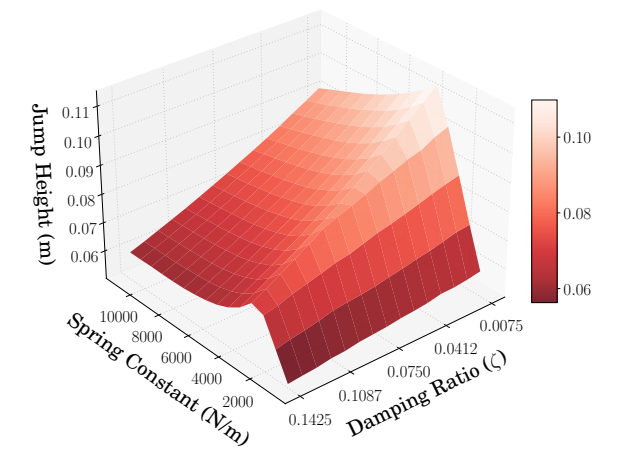


Fig. 7. Height Jumped Given Non-close to Optimal Range of Design Parameters

design space to choose from that was not close to optimal, two different cases were tested. For the first case, the agents were provided with a set of designs where a varied range of designs could meet the performance requirements. For the second case, the agents were provided with a design space to select from where more specific design parameters were needed to meet optimal performance.

The number of learning steps that were performed was 1000, with the first 100 being rollout steps. This provided the agents, in both cases previously mentioned, enough learning time to converge to designs that satisfied the performance requirements. During the training process, the height reached during the simulation phase (per environment step) and the design parameters selected by the algorithm where collected to evaluate the learning process. The results are presented in the next section.

VI. JUMPING HEIGHT REACHED

A. Evaluation Technique

To evaluate the usability of RL for finding high performing design parameters, the performance of the design parameters the agents had access to were plotted and are presented

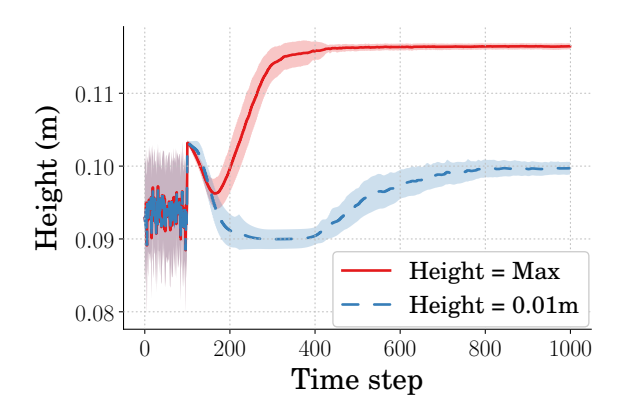


Fig. 8. Height Reached During Training

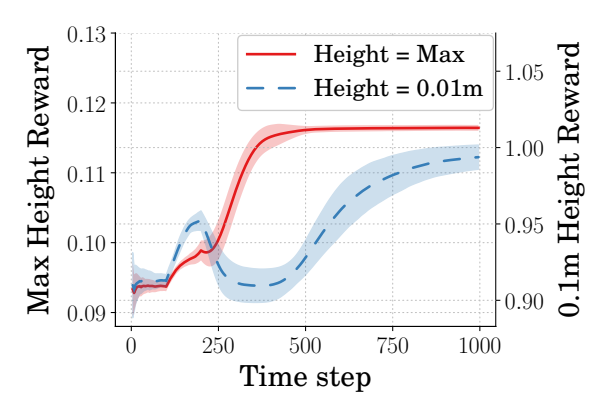


Fig. 9. Reward Received During Training

in Figures 6 and 7. Figure 6 represents the heights the pogo-stick could reach where changes in the damping ratio constant had little effect on design performance. Therefore, the design space provided to the agent in this case is close to optimal in terms of damping ratio. Similarly, Figure 7 represents the heights the pogo-stick could reach. However, in this case, changes to the damping ratio constant have a greater effect on jumping performance creating a design space which is farther from optimal.

B. Design Learned Given Close to Optimal Design Parameters

Figures 8 and 9 show the height achieved by the learned designs, and the reward received during training, both for the agents given a close to optimal design space. For the agents learning designs to maximize jump height, Figure 8 can be compared with Figure 6 showing that the agent learned a design nearing one which would achieve maximum performance. Additionally, looking at the agents learning designs to jump to the specified 0.01 meters, the designs learned accomplish this with slightly more variance than that of the max height case. Figure 9 shows the rewards the agents received during training and support that both agent types learned designs which converged.

The average and standard deviation of the spring constant and damping ratio design parameters the agents selected during training are shown in Figures 10 and 11. These plots represents the learning curves for the agents learning

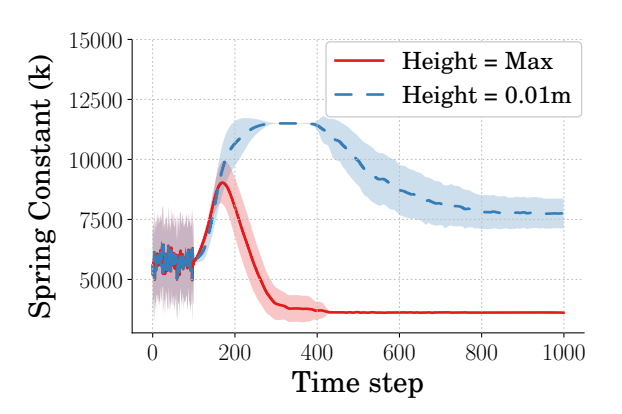


Fig. 10. Spring Constant Selected During Training

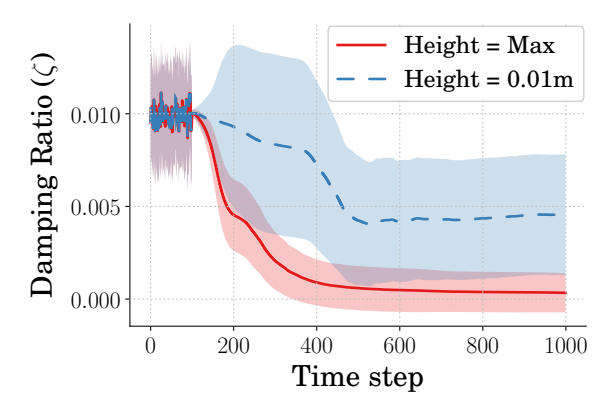


Fig. 11. Zeta Value Selected During Training

design parameters to maximize jump height and the agents learning design parameters to jump to 0.01m. Additionally, these represent the designs the agent selected given a close to optimal design space. Looking at the agents that learned designs to jump to a specified height, it can be seen that there is a high variance in both the spring constant and the damping ratio found. The agents which were learning designs which maximized height found designs with very little variance in terms of spring constant and significantly less variances in terms of damping ratio.

C. Given Non-close to Optimal Design Parameters

Figures 12 and 13 show the height achieved by the learned designs, and the reward received during training, both for the agents given a design space which was not close to optimal. For the agents learning designs to maximize jump height, Figure 12 can be compared with Figure 7 showing that the agents learned a design nearing one which would achieve maximum performance. Additionally, looking at the agents learning designs to jump to the specified 0.01 meters, the designs learned accomplish this, only with slightly more variance than what is seen in the maximum agents. Figure 13 shows the rewards the agents received during training and support that both agent types learned designs which converged. In this cas though, the agent learning a specific design requires more learning steps to converge.

The average and standard deviation of the spring constant and damping ratio design parameters the agents selected

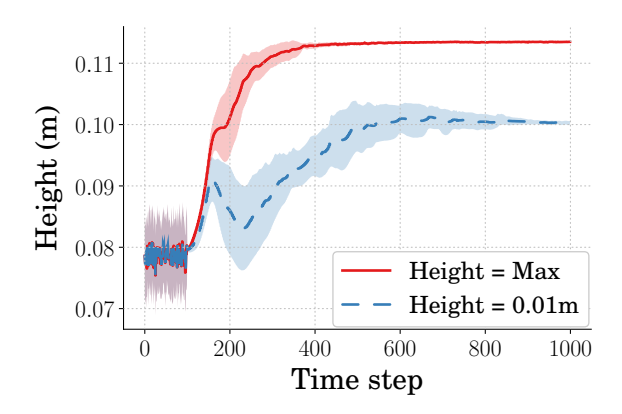


Fig. 12. Height Reached During Training

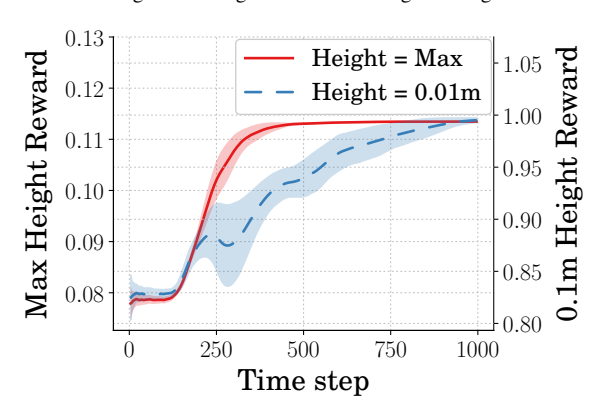


Fig. 13. Reward Received During Training

during training are shown in Figures 14 and 15. These plots represents the learning curves for the agents learning design parameters to maximize jump height and the agents learning design parameters to jump to 0.01m. Additionally, these represent the designs the agents selected given a design space to choose from which was farther from optimal. Looking at the agents that learned designs to jump to a specified height, it can be seen that there is a high variance in spring constant throughout training, however the majority of agents converge to a specific design lowering the variance. The same can be seen in the damping ratio, however the variance is mitigated significantly earlier in training. The agents which were learning designs that maximized height found them with very little variance in terms of spring constant and damping ratio.

D. Average Design Performance

The final mean and standard deviation of the design parameters for the two different cases are presented in Table III. In the case where the agent learns parameters using a design space that is not close to optimal, the agent learns designs with less variance both for spring constant and for damping ratio. Figure 16 shows the jumping performance of the mean designs learned for both cases tested. Designs that satisfied the constraint with minimal error were found by the agents tasked with learning parameters to reach the specified 0.01 meters. The difference seen in maximum height reached between the two cases represents the difference in the damping

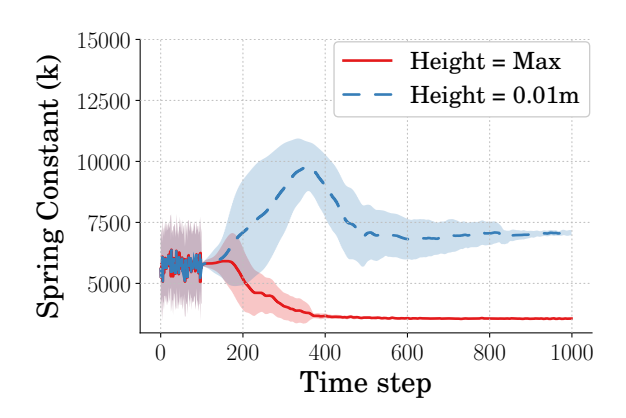


Fig. 14. Spring Constant Selected During Training

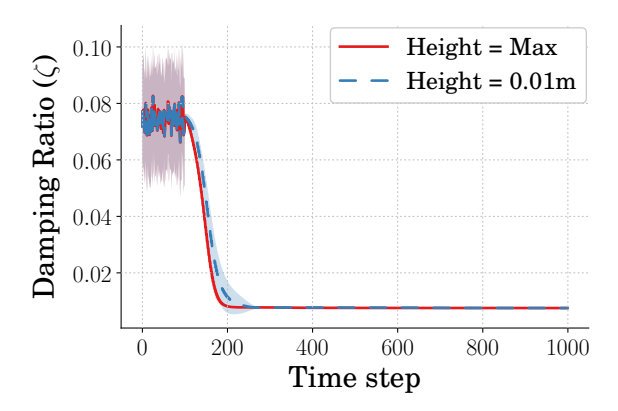


Fig. 15. Zeta Value Selected During Training

ratio design space the agents had access to. Regardless, the peak heights achieved can be compared again to Figures 6 and 7 to show that the agents learned designs nearing those achieving maximum performance.

VII. CONCLUSION

The pogo-stick model was used in conjunction with a predetermined control input to determine if a reinforcement learning algorithm (TD3) could be used to find optimal performing design parameters regarding jumping performance. This work was done in part to determine if RL could be used as the mechanical design learner for an intelligent

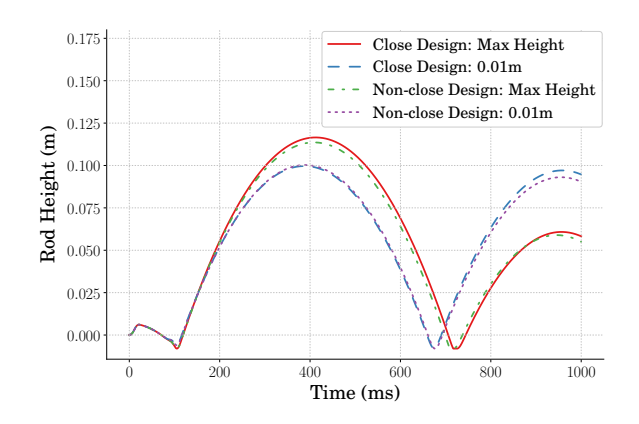


Fig. 16. Height vs Time of Average Optimal Designs

TABLE III
LEARNED DESIGN PARAMETERS

Training Case		Design Parameter	Mean	STD
Close to Optimal Design	Learn Max Height	Spring Constant	3.62e03	3.82e01
		Damping Ratio	3.37e-04	2.11e-03
	Learn Specified Height	Spring Constant	7.74e03	1.24e03
		Damping Ratio	4.55e-03	6.49e-03
Non-Close to Optimal Design	Learn Max Height	Spring Constant	3.55e03	4.86e01
		Damping Ratio	7.53e-03	8.86e-06
	Learn Specified Height	Spring Constant	7.07e03	2.16e02
		Damping Ratio	7.54e-03	3.27e-05

concurrent design algorithm. It was shown that when providing an agent with design parameters to choose from which were close to optimal, the agents performed well in finding design parameters which met the performance constraints. The designs found were high in design variance however. It was additionally shown that when provided with design parameters which were not close to optimal, the agents excelled at finding design parameters which were lower in design variance but still met the design constraints.

ACKNOWLEDGMENT

The authors would like to thank the Louisiana Crawfish Promotion and Research Board for their support of this work.

REFERENCES

- [1] Y. Sugiyama and S. Hirai, "Crawling and jumping of deformable soft robot," 2004 IEEE/RSJ International Conference on Intelligent Robots and Systems (IROS), vol. 4, no. c, pp. 3276–3281, 2004.
- [2] G. Buondonno, J. Carpentier, G. Saurel, N. Mansard, A. De Luca, and J. P. Laumond, "Actuator design of compliant walkers via optimal control," *IEEE International Conference on Intelligent Robots and Systems*, vol. 2017-Septe, pp. 705–711, 2017.
- [3] J. Hurst, "The Role and Implementation of Compliance in Legged Locomotion," *The International Journal of Robotics Research*, vol. 25, no. 4, p. 110, 2008.
- [4] T. Zhang and H. Huang, "Design and Control of a Series Elastic Actuator with Clutch for Hip Exoskeleton for Precise Assistive Magnitude and Timing Control and Improved Mechanical Safety," *IEEE/ASME Transactions on Mechatronics*, vol. 24, no. 5, pp. 2215–2226, 2019.
- [5] G. A. Pratt and M. M. Williamson, "Series elastic actuators," *IEEE International Conference on Intelligent Robots and Systems*, vol. 1, pp. 399–406, 1995.
- [6] F. Iida, G. Gómez, and R. Pfeifer, "Exploiting body dynamics for controlling a running quadruped robot," 2005 International Conference on Advanced Robotics, ICAR '05, Proceedings, vol. 2005, pp. 229– 235, 2005.
- [7] U. Saranli, M. Buehler, and D. E. Koditschek, "RHex: A Simple and Highly Mobile Robot," *International Journal of Robotics Research*, vol. 20, no. 7, pp. 616–631, 2001.
- [8] Z.-h. Luo, "Direct Strain Feedback Control of Flexible Robot Arms: New Theoretical and Experimental Results," vol. 38, no. 11, 1993.
- [9] A. M. Modeling, "Gain Adaptive Nonlinear Feedback Control of Flexible SCARA / Cartesian Robots," no. AIM, pp. 1423–1428, 2003.
- [10] S. Bhagat, H. Banerjee, Z. T. H. Tse, and H. Ren, "Deep reinforcement learning for soft, flexible robots: Brief review with impending challenges," *Robotics*, vol. 8, no. 1, pp. 1–36, 2019.
- [11] T. G. Thuruthel, E. Falotico, F. Renda, and C. Laschi, "Model Based Reinforcement Learning for Closed Loop Dynamic Control of Soft Robotic Manipulators," *IEEE Transactions on Robotics*, vol. 35, pp. 124–134, 2019.
- [12] Z. Dwiel, M. Candadai, and M. Phielipp, "On Training Flexible Robots using Deep Reinforcement Learning," *IEEE International Conference* on *Intelligent Robots and Systems*, pp. 4666–4671, 2019.
- [13] D. Ha, "Reinforcement learning for improving agent design," Artificial Life, vol. 25, no. 4, pp. 352–365, 2019.

- [14] T. Chen, Z. He, and M. Ciocarlie, "Hardware as Policy: Mechanical and computational co-optimization using deep reinforcement learning," arXiv, no. CoRL, 2020.
- [15] C. Schaff, D. Yunis, A. Chakrabarti, and M. R. Walter, "Jointly learning to construct and control agents using deep reinforcement learning," *Proceedings - IEEE International Conference on Robotics* and Automation, vol. 2019-May, pp. 9798–9805, 2019.
- [16] M. Ahmadi and M. Buehler, "Stable control of a simulated one-legged running robot with hip and leg compliance," *IEEE Transactions on Robotics and Automation*, vol. 13, no. 1, pp. 96–104, 1997.
- [17] W. He, H. Gao, C. Zhou, C. Yang, and Z. Li, "Reinforcement Learning Control of a Flexible Two-Link Manipulator: An Experimental Investigation," *IEEE Transactions on Systems, Man, and Cybernetics: Systems*, pp. 1–11, 2020.
- [18] T. P. Lillicrap, J. J. Hunt, A. Pritzel, N. Heess, T. Erez, Y. Tassa, D. Silver, and D. Wierstra, "Continuous control with deep reinforcement learning," 4th International Conference on Learning Representations, ICLR 2016 Conference Track Proceedings, 2016.
- [19] Q. Li, W. J. Zhang, and L. Chen, "Design for control A concurrent engineering approach for mechatronic systems design," *IEEE/ASME Transactions on Mechatronics*, vol. 6, no. 2, pp. 161–169, 2001.
- [20] T. Wang, Y. Zhou, S. Fidler, and J. Ba, "Neural graph evolution: Towards efficient automatic robot design," arXiv, pp. 1–17, 2019.
- [21] R. Blickhan and R. J. Full, "Similarity in multilegged locomotion: Bouncing like a monopode," *Journal of Comparative Physiology A*, vol. 173, no. 5, pp. 509–517, 1993.
- [22] K. L. Sorensen and W. E. Singhose, "Command-induced vibration analysis using input shaping principles," Automatica, vol. 44, no. 9, pp. 2392 2397, 2008, analysis tools; Analytical tools; Command shaping; Deconvolution; Dynamic Systems; Induced vibrations; Input shaping; Key systems; Performance analyses; Phase plane; Residual vibrations; Simple methods; Vector diagram; Vibration analysis; Vibratory response; [Online]. Available: http://dx.doi.org/10.1016/j.automatica.2008.01.029
- [23] N. C. Singer and W. P. Seering, "Preshaping command inputs to reduce system vibration," *Journal of Dynamic Systems, Measurement, and Control*, vol. 112, pp. 76–82, March 1990.
- [24] W. Singhose, W. Seering, and N. Singer, "Residual vibration reduction using vector diagrams to generate shaped inputs," ASME J. of Mechanical Design, vol. 116, pp. 654–659, June 1994.
- [25] J. Vaughan, "Jumping Commands For Flexible-Legged Robots," 2013.
- [26] S. Fujimoto, H. Van Hoof, and D. Meger, "Addressing Function Approximation Error in Actor-Critic Methods," 35th International Conference on Machine Learning, ICML 2018, vol. 4, pp. 2587–2601, 2018
- [27] G. Brockman, V. Cheung, L. Pettersson, J. Schneider, J. Schulman, J. Tang, and W. Zaremba, "OpenAI Gym," pp. 1–4, 2016. [Online]. Available: http://arxiv.org/abs/1606.01540